HYDROLOGICAL PROCESSES
Hydrol. Process. **17**, 2171–2193 (2003)
Published online in Wiley InterScience (www.interscience.wiley.com). DOI: 10.1002/hyp.1327

Predicting space–time variability of hourly streamflow and the role of climate seasonality: Mahurangi Catchment, New Zealand

S. E. Atkinson,[1] M. Sivapalan,[1]* N. R. Viney[2] and R. A. Woods[3]

[1] *Centre for Water Research, The University of Western Australia, 35 Stirling Highway, Crawley, WA 6009, Australia*
[2] *CSIRO Land and Water, Private Bag, No. 5, Wembley, WA 6913, Australia*
[3] *National Institute of Water and Atmospheric Research Ltd, PO Box 8602, Christchurch, New Zealand*

Abstract:

We present a systematic approach to achieving accurate hourly streamflow predictions at locations internal to a catchment, potentially with minimal calibration. Each step in this approach is meant to provide insight into the relative importance of catchment and climatic properties (rainfall, soil, vegetation, topography), their spatial variability, and their influence on the spatial and temporal variability of streamflows. This has been made possible through the use of a simple conceptual model design requiring minimal calibration and with physically meaningful catchment parameters estimated mostly *a priori* from landscape data, and climatic variables. Eight model types originating from this simple conceptual model design, with complexity ranging from lumped to fully distributed, were tested over summer and winter periods at the Mahurangi Catchment, New Zealand, and the preferred model identified using statistical assessment criteria. Results of the simulations suggest that, although the required model complexity was found to be a function of the season (summer versus winter), a fully distributed representation is most appropriate for accurate predictions under all seasonal climate conditions. Using this model, the success of hourly flow predictions in space–time was assessed and sensitivity analysis used to identify the dominant controls on the timing and magnitude of hourly flow predictions and to investigate the adequacy of the assumption of homogeneity for a number of catchment properties. Copyright © 2003 John Wiley & Sons, Ltd.

KEY WORDS streamflow; predictions; climate; space–time variability; dominant controls; seasonality; models

INTRODUCTION

There are numerous distributed models capable of predicting the space–time variability of the streamflow response at the catchment scale (Abbott *et al*., 1986; Moore and Grayson, 1991). Although successful in many applications, because of model complexity and the bottom-up procedure by which these models have been constructed, they do not readily provide the modeller with physical insights into the dominant controls on streamflow variability. The minimum model complexity required for accurate predictions for given applications or at given space or time scales also cannot be readily assessed. This understanding is essential if inroads are to be made against the problem of predicting streamflow in ungauged basins.

Our previous work (Jothityangkoon *et al*., 2001; Atkinson *et al*., 2002, 2003; Farmer *et al*., 2003; Eder *et al*., 2003), using Klemes' (1983) *downward* (or *top-down*) *approach*, has found the model complexity required for accurate predictions of streamflow at the outlet of a catchment to be a function of climate and time scale. However, this work did not extend to an investigation of the model complexity required for predictions of internal flow variability, at locations within the catchment. Atkinson *et al*. (2003) made use of detailed datasets assembled as part of the MARVEX field experiment (Woods *et al*., 2001) to predict and

* Correspondence to: M. Sivapalan, Centre for Water Research, The University of Western Australia, 35 Stirling Highway, Crawley, WA 6009, Australia. E-mail: sivapalan@cwr.uwa.edu.au

Received 15 December 2002
Accepted 28 February 2003

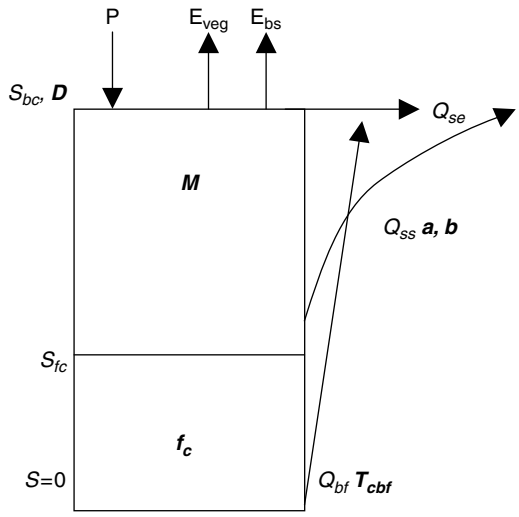

Figure 1. Operations of simple storage model (Atkinson *et al*., 2002a). Symbols are defined Appendix A

Table I. Attributes of tested Models A–H

Attribute	A	B	C	D	E	F	G	H
Uniform rainfall	√		√	√			√	
Uniform catchment parameters	√	√		√		√		
Single store	√	√	√		√			
Spatially variable rainfall		√			√	√		√
Spatially variable catchment parameters			√		√		√	√
Multiple buckets				√		√	√	√
Number of input parameters	7	7	88	8	88	8	89	89

test hourly predictions of streamflows at the outlet of the 47 km^2 Mahurangi Catchment, New Zealand, using models ranging from lumped to fully distributed and configured from the same simple model design depicted in Figure 1. The attributes of these models have been listed in Table I and incorporate either uniform or distributed values of hourly rainfall, uniform or distributed catchment parameters and single or multiple buckets (representing storage), with all remaining parameters assumed to be homogeneous. Although testing models with different complexities does not identify one distinct path that should be taken when identifying the most suitable model design (often assumed when using the 'downward approach'), comparing the results of simple models against more complex models allows us to deduce the accuracy of models resulting from increasing complexity and helps us to make the connection between climate controls, time scale and model performance. In particular, Atkinson *et al*. (2003) investigated the dominant controls on the timing and magnitude of hourly flow predictions at the outlet, finding that the parameters representing soil depth, soil hydraulic properties and network routing had the most influence. In addition, through sensitivity analysis, they showed that the assumption of spatial homogeneity of many of the catchment attributes is sufficient for lumped predictions at the outlet. No attempt was made to look in any great detail at seasonal differences in the required model complexity, seasonal differences in the dominant controls on flow variability, or the accuracy of internal hourly flow predictions.

Given that summer and winter storms represent the two most extreme climatic conditions experienced throughout the year at the Mahurangi Catchment, (i.e. storms occurring under dry and wet conditions respectively), in this paper the adequacy of the eight model types in Table I, for making accurate space–time

predictions of streamflows, is tested over one summer and one winter period (each of 5 days duration). Results reported by Atkinson *et al*. (2002b) suggested there were significant seasonal differences in the catchment response between summer and winter. Therefore, the differences in model complexity required to predict variability of stormflow volumes between summer and winter events are also investigated (stormflow volume being defined as the total volume of flow generated within the boundary of an individual subcatchment over a defined period, in this case the duration of the storm event). Sensitivity analysis is also performed to identify the dominant controls on streamflow variability, any seasonal change in these dominant controls and the sources of error in any unsatisfactory predictions of the volume or timing of hourly flow. With the understanding gained, the adequacy of the assumption of homogeneity of a number of catchment properties is investigated and recommendations made as to the minimum model complexity required for accurate internal predictions of hourly streamflow. At every step the paper reflects our desire, consistent with the downward approach, for a comprehensive analysis of observed data, and the interpretation of observed patterns in space and time therein, through modelling carried out in a systematic and hierarchical manner.

SITE DESCRIPTION

The Mahurangi Catchment covers an area of approximately 47 km^2 in the North Island of New Zealand (Figure 2), and is the focus of an ongoing collaborative research programme aimed at investigating the space–time variability of catchment water balance. This programme, known as MARVEX (the Mahurangi River Variability Experiment), has collected essential data required to identify the causes of variability in streamflow and soil moisture at different spatial and temporal scales, through an intensive hydrological measurement network (Woods *et al*., 2001). The Mahurangi Catchment has an average annual rainfall of 1628 mm, average annual potential evaporation E_p of 1315 mm and an average annual streamflow of 842 mm.

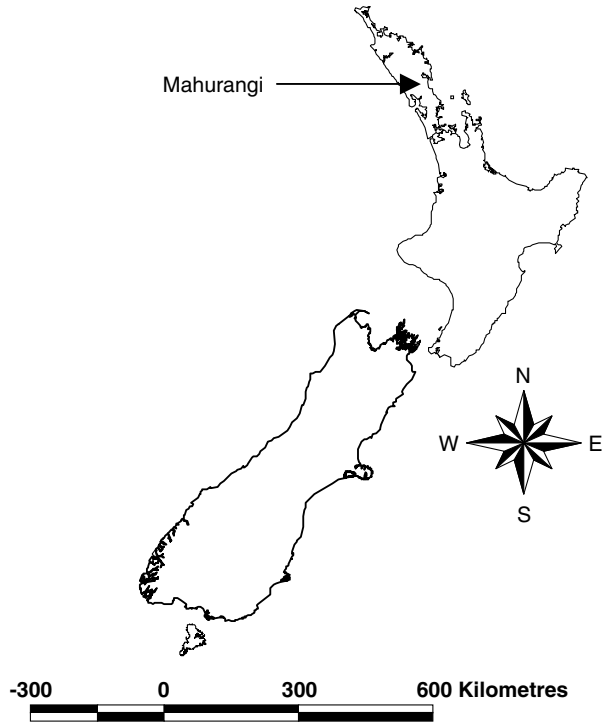

Figure 2. Location of the Mahurangi Catchment, New Zealand

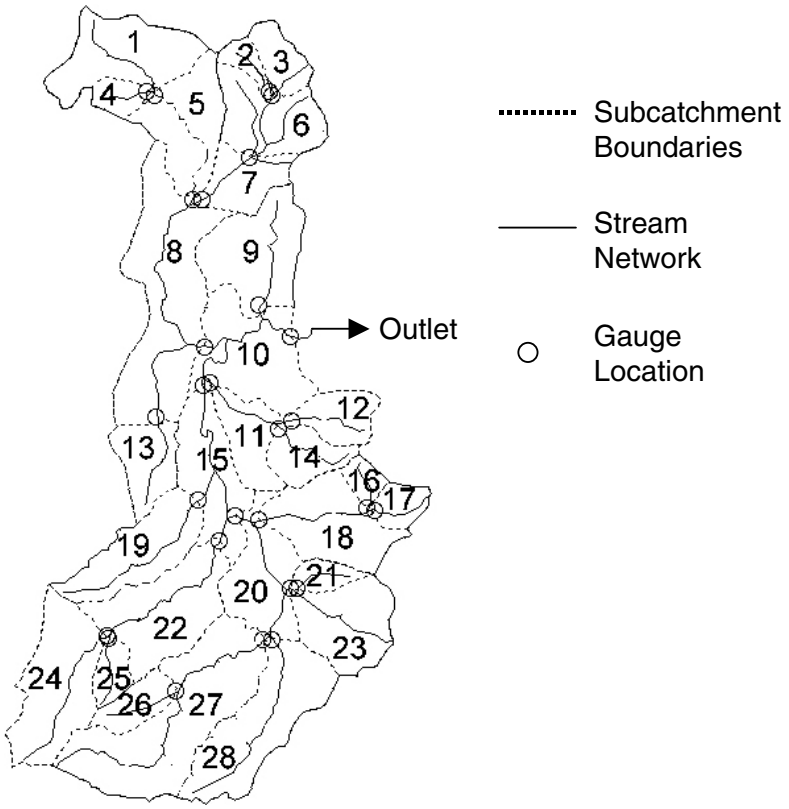

Figure 3. The Mahurangi Catchment divided into 28 subcatchments (broken line) and the location of the 28 gauging stations (open circles)

As shown in Figure 3, the catchment was divided into 28 subcatchments based on the locations of the stream gauges, each with its own detailed database of fractional forest cover M, field capacity θ_{fc}, soil depth D, permanent wilting point θ_{pwp}, porosity ϕ and streamflow. As seen in Figure 3, subcatchments are defined by the parts of the catchment located between gauges. Hourly rainfall was estimated for the entire catchment and for each individual subcatchment using the Thiessen polygon method using rainfall measured at 12 locations in and near the catchment, and the hourly potential evaporation was assumed to be uniform across the catchment, and was estimated based on one Class-A evaporation pan located at the outlet. Streamflows recorded at the 28 gauging stations depicted in Figure 3 were used to test model predictions of hourly flows.

In this study, two 5-day storms were analysed: one in summer (3–7 December 1998) (December 1998) and the other in winter (10–14 August 1998). The rainfall and potential evaporation over these periods were 40·1 mm and 17·5 mm respectively over the summer period and 112·3 mm and 6·1 mm respectively over the winter period.

Reliability of streamflow records

As the MARVEX experiment was not a flood study, the temporary weirs installed across the catchment are small and are not accurate during high flow events. Logger failure or the failure of weirs by flood damage resulted in periods of missing streamflow records, which were filled in by extrapolation from nearby gauging stations using the method of matching flow duration curves (Hughes and Smakhtin, 1996; Ibbitt and Henderson, 1998). The gauging station located at the catchment outlet (see Figure 3) is permanent and provides reliable streamflow records even during floods. Of the remaining 27 gauges installed within the

catchment, a number of gauges required data filling using correlation with nearby flow recorders. Over the summer period (3–7 December 1998) gauges 2, 3, 4, 7, 18, 24 and 26 required filling, whereas over the winter period (10–14 August 1998) gauges 2, 4, 7, 18, 20, 21, 23, 24, 25 and 26 required filling. Independent tests indicate that the synthesized data for these sites will be within ±20% of the observed value for about 80% of the time (R. P. Ibbitt, personal communication, 2000). Although few in number, these inconsistencies have had a major impact on the results presented in this paper. Suspect periods have been omitted from statistical analysis where possible; however, this is a subjective procedure and so has not been used extensively.

MODEL DESIGNS

Basic model structure: building block of downward approach

The basic model structure depicted in Figure 1 is used as the building block for further model development and hourly flow predictions in space and time. All relevant symbols and equations are presented in Appendix A. The model is nominally conceptual, requiring hourly inputs of rainfall, potential evaporation and mostly *a priori* estimates of lumped, but physically meaningful input parameters (a, T_{cbf}, S_{bc}, M and f_c), and only minimal calibration with streamflow records is required. In this paper, following Atkinson *et al.* (2003), the interception process was added to the basic model structure (and thus all models in Table I) through introduction of an overflow interception store. The capacity of this store for fully forested subcatchments is denoted by S_{bcint}. This parameter S_{bcint} is estimated such as to match the average fraction of annual rainfall that is intercepted by the dominant vegetation type, when fully forested. For *Pinus radiata* (prevalent vegetation type within Mahurangi) the annual interception loss is 25% of annual rainfall (Duncan, 1995), and S_{bcint} is chosen such as to produce this magnitude of annual interception loss. In subcatchments with partial forest cover, the capacity of the interception store is the estimated full forest value S_{bcint} multiplied by M (a 50% cleared catchment, $M = 0{\cdot}5$, would have an interception capacity of $0{\cdot}5S_{bcint}$). The relevant equations are provided in Appendix A.

To make predictions of hourly streamflow at different locations within the catchment, each of the 28 subcatchments depicted in Figure 3 is modelled separately and the runoff volumes estimated by the model for each subcatchment are deposited in the adjacent channel and routed to the outlet via the constant-velocity algorithm of Viney and Sivapalan (1995). This routing algorithm requires a constant velocity parameter V, estimated to be $0{\cdot}5$ m s^{-1}, based on calibration against observed streamflow records at the outlet (Atkinson *et al.*, 2003). This parameter can also be estimated accurately from field measurements and, in principle, can be estimated without calibration. The recession parameters a (Wittenberg and Sivapalan, 1999) and T_{cbf} (a measure of subsurface travel time) are assumed homogeneous across the catchment for all model simulations. The method used to determine these parameter values is presented in Atkinson *et al.* (2002, 2003), and all relevant equations are provided in Appendix A.

Each model listed in Table I uses different combinations of uniform or variable rainfall, uniform or variable catchment parameters (f_c, S_{bc} and M), and either a single bucket or multiple buckets to represent soil water storage. Details of these model components and how they are applied in uniform, semi-distributed and fully distributed fashion are now described in detail.

Rainfall inputs

Rainfall can be applied in two ways: (1) constant in space and (2) spatially variable. If the rainfall is assumed to be spatially variable then the Thiessen polygon method may be used to estimate the rainfall time series for the respective subcatchments. If we assume the rainfall intensity is uniform (between subcatchments) then the catchment average rainfall estimated by the Thiessen polygons using rainfall recorded at all 12 raingauges is applied to the entire catchment.

Catchment properties

As with rainfall, catchment properties can be applied in two ways: (1) constant in space and (2) spatially variable. Under all circumstances, and as mentioned before, the parameters describing subsurface flow and baseflow recessions (a and T_{cbf}) and the parameter representing the interception capacity S_{bcint} remain constant in space. The remaining parameters describing soil properties (S_{bc}, f_c) and the fractional forest cover M can be represented as either catchment average values or can be estimated individually for each subcatchment. The catchment average values are presented in Table II and the estimates for each individual subcatchment are provided in Table III. Both datasets were estimated through field measurement of soil properties (porosity, field capacity, soil depth and permanent wilting point) at various locations across the catchment and through aerial photographs of vegetation cover. The inclusion of spatially variable catchment properties alone increases the number of parameter values from seven in Model A to 88 in Model C (Table I).

Multiple buckets and partial area runoff generation

To incorporate a distributed hillslope representation using multiple buckets, each subcatchment is represented by a number of buckets with varying capacities S_{bc} acting in parallel. To describe the distribution of buckets, we assign an additional dimensionless empirical parameter β, assumed to be spatially uniform (between subcatchments). Following Zhao *et al*. (1980), these bucket capacities are assumed to belong to the Xinanjiang distribution (cumulative distribution function) given by

$$F_{SB}(SB) = 1 - (1 - SB)^{\beta} \tag{1}$$

where SB is the dimensionless ratio of bucket capacity S_{bc} to the maximum bucket capacity within the subcatchment S_{bcmax}. Manipulation of Equation (1) leads to a simple expression for the mean ratio SB_{mean} as a function of β only:

$$SB_{mean} = \frac{S_{bcmean}}{S_{bcmax}} = \frac{1}{1+\beta} \tag{2}$$

In principle, β can be estimated from existing data on spatial variability of soil depth and porosity. However, to our knowledge, few studies have been conducted where the value of β has been estimated directly from field data, and this type of information was also not available at Mahurangi; so, as described by Atkinson *et al*. (2003), β was varied over the accepted range of $0{\cdot}05 < \beta < 5$ to identify the value for which the model produced an amount of saturation excess runoff matching field observations.

Field observations suggest that, over the period spanning 1 March 1998 to 1 March 1999, 25% of the total annual runoff was generated by saturation excess (T. Chirico, personal communication, 2000; M. J. Duncan, personal communication, 2000). The results of sensitivity analysis performed by Atkinson *et al*. (2003) suggested that $\beta = 0{\cdot}5$ provided the most accurate model predictions of saturation excess runoff produced from

Table II. Catchment average parameter values

Parameter	Value
M	0·44
f_c	0·53
S_{bc} (mm)	189·8
a (mm^{1-b} h^b)	75
T_{cbf} (h)	2000
S_{bcini} (mm)	4·1
V (m s^{-1})	0·5
β	0·5

Table III. Soil and vegetation properties for each individual subcatchment

Catchment	M	S_{bc} (mm)	f_c
1	0·10	200	0·48
2	0·14	188	0·47
3	1·00	190	0·51
4	0·60	191	0·57
5	0·70	216	0·58
6	0·38	192	0·58
7	0·10	167	0·63
8	0·45	202	0·70
9	0·34	195	0·67
10	0·18	181	0·69
11	0·10	184	0·57
12	0·10	182	0·56
13	0·22	186	0·52
14	0·16	188	0·50
15	0·19	196	0·49
16	0·54	199	0·48
17	0·57	181	0·48
18	0·39	199	0·48
19	0·85	187	0·49
20	0·89	186	0·50
21	0·85	188	0·50
22	0·61	196	0·49
23	0·32	188	0·52
24	0·45	190	0·51
25	0·20	182	0·47
26	0·40	184	0·46
27	0·46	199	0·52
28	1·00	189	0·51

the catchment (24%). Given field measurements of mean soil depth at various locations across the catchment we are able to estimate the mean bucket capacity S_{bcmean} using Equation (A.1), and then use Equation (2), β and S_{bcmean} to estimate the mean ratio SB_{mean} and the maximum bucket capacity S_{bcmax}.

ASSESSMENT CRITERIA

The assessment criteria used to compare model predictions are taken from Ye *et al.* (1997). These are the absolute mean deviation A, mean bias B, efficiency E, and correlation coefficient ρ, as defined in Equations (3)–(6) respectively:

$$A = n^{-1} \sum_{j=1}^{n} |q_{\text{p}_j} - q_{\text{o}_j}| \tag{3}$$

$$B = n^{-1} \sum_{j=1}^{n} (q_{\text{p}_j} - q_{\text{o}_j}) = n^{-1} \sum_{j=1}^{n} e_j \tag{4}$$

$$E = 1 - \frac{\mu_{\text{e}}^2}{\sigma_{\text{o}}^2} \tag{5}$$

$$\rho = \frac{\mathrm{cov}_{\mathrm{p,o}}}{\sqrt{\sigma_{\mathrm{p}}^2 \sigma_{\mathrm{o}}^2}} \tag{6}$$

These criteria can be used to compare spatial patterns of cumulative stormflow volumes from subcatchments, or to compare the observed and model predicted time series of streamflows at a single site (in which case they are denoted with asterisks, i.e. A^*, B^*, E^* and ρ^*). In the above, the term μ_{e}^2 is the second moment of the residuals $e_j = q_{\mathrm{p}} - q_{\mathrm{o}}$ between predicted discharge q_{p} and observed discharge q_{o}. The terms σ_{o}^2 and σ_{p}^2 are the variances of the observed and predicted discharges respectively, $\mathrm{cov}_{\mathrm{p,o}}$ is the covariance between the observed and predicted discharges, and n is the number of observations (length of time series, or number of subcatchments).

RESULTS AND DISCUSSION

Spatial patterns of observed stormflow volumes in winter and summer

Using the observed streamflow records, stormflow volumes from each subcatchment are estimated over both summer and winter periods. The results are presented in Figure 4. Several of the streamflow records in both the summer and winter periods used in this study have some periods of missing data, and were filled using methods already described. Data for those sites are less reliable than for sites with complete flow records. Subcatchment stormflow volumes are estimated using differences between flows at gauging stations, and thus have larger uncertainties than flows at individual gauging stations. This uncertainty is also larger for subcatchments that contribute only a small fraction of the flow at the downstream gauging station. Poor streamflow records at upstream and/or downstream gauging stations sometimes produced stormflow volumes that exceeded the total rainfall. When this occurred, the subcatchment was omitted from further analysis. Stormflow volume calculations for subcatchments 7, 10 and 20 over the summer period and subcatchments 5, 10, 15, 20, 23 and 24 over the winter period demonstrated such deficiencies, and have been omitted from the analysis.

Comparison of the spatial patterns of total rainfall and stormflow volumes over both the summer and winter periods highlights significant seasonal differences in catchment response. For the summer storm selected for study here (Figure 4a), the rainfall is quite uniform across the catchment, whereas the observed stormflow volume is comparatively more variable. Conversely, the winter storm had both variable rainfall (compared with the summer storm) and variable runoff volume (Figure 4b). Correlation between observed spatial patterns of winter rainfall and stormflow volume was found to be 0·35, whereas for the summer storms the correlation was only 0·10. This suggests that, although variability in rainfall is not the single most important influence on observed variability of stormflow volume, there is a stronger influence in winter than in summer. These trends are explained by the characteristic antecedent conditions of summer and winter storms. Soils are typically much drier in summer because of greater evaporation rates and less frequent rainfall, and the small rainfall total in this storm mainly acts to replenish the storage deficit rather than to produce immediate runoff. In addition, as mentioned before, the spatial variability of rainfall is low in the storm studied. These two factors help explain the weak correlations shown in Figure 4a. In contrast, the catchment is more responsive to rainfall in winter storms, and any (even if small) rainfall variability is more readily transferred through to streamflows.

Summer and winter predictions of stormflow volume

The performance measures for simulations of stormflow volumes using the eight models in Table I are presented in Tables IV and V for the winter and summer periods respectively, and provide a direct comparison of observed and predicted spatial patterns. Note that A, B and E measure the ability of the models to predict stormflow volumes accurately, whereas ρ is a measure of the ability to predict spatial patterns, and, in this

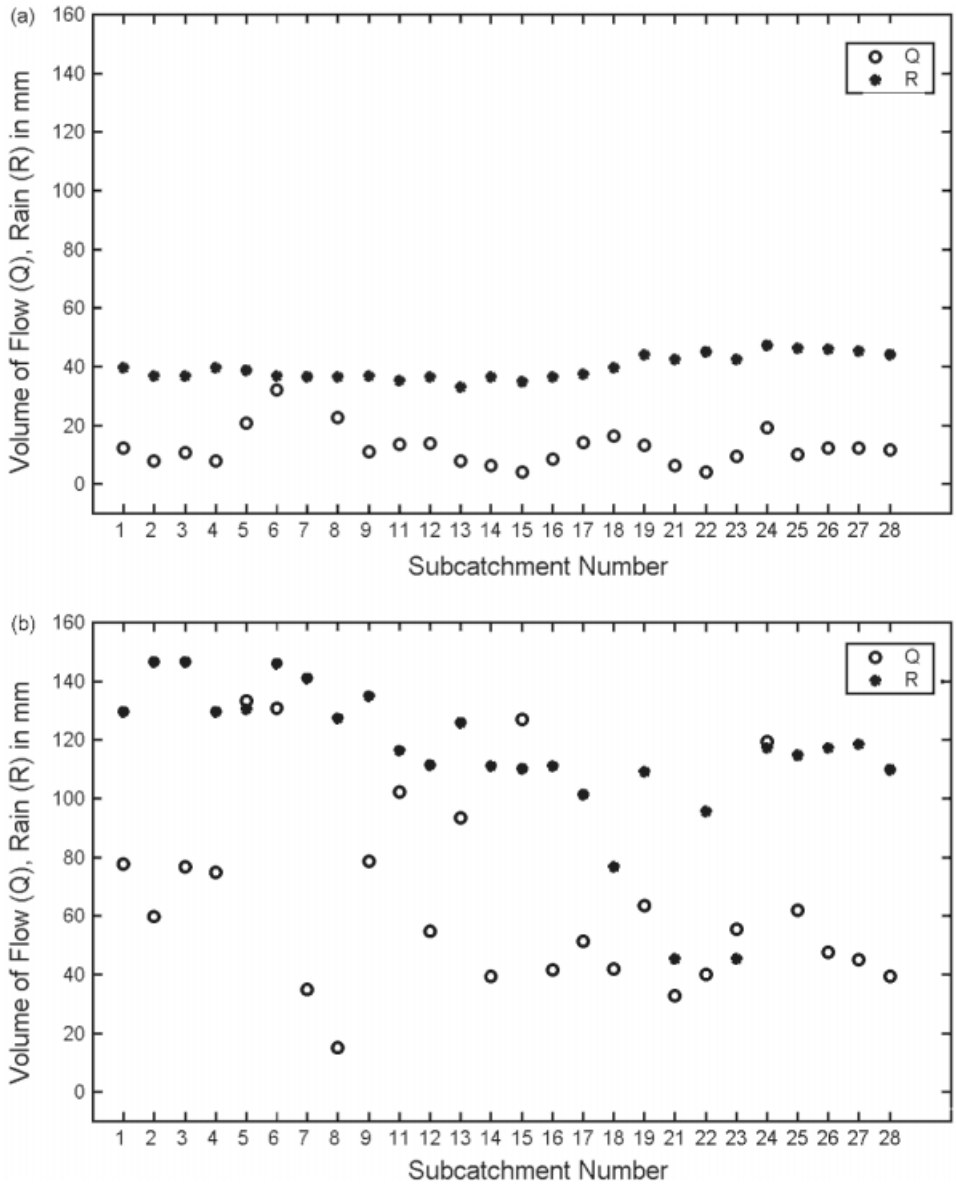

Figure 4. Observed stormflow Q and total rainfall R for (a) summer and (b) winter periods

Table IV. Goodness of fit statistics for the spatial patterns for winter period stormflow volumes (10–14 August 1998)

Assessment criteria	Model A	Model B	Model C	Model D	Model E	Model F	Model G	Model H
A (mm)	26·327	24·142	25·959	27·428	24·196	25·662	27·191	25·257
B (mm)	−2·992	0·809	−2·027	2·286	1·752	4·941	2·633	5·573
E	−0·019	0·067	0·004	0·004	0·030	0·060	0·006	0·040
ρ	Undefined	0·319	−0·084	Undefined	0·313	0·328	−0·136	0·332

Table V. Goodness of fit statistics for the spatial patterns for winter period stormflow volumes (10–14 August 1998)

Assessment criteria	Model A	Model B	Model C	Model D	Model E	Model F	Model G	Model H
A (mm)	7·327	7·491	7·616	6·139	6·909	6·420	6·450	5·955
B (mm)	−4·297	−2·040	−3·022	−1·978	−2·925	−0·905	−1·393	−1·450
E	−0·144	−0·008	−0·227	0·002	0·051	0·120	−0·057	0·155
ρ	Undefined	0·260	−0·135	Undefined	0·321	0·314	−0·105	0·428

instance, it is the critical statistic. It should be noted that as Model A produces the same volume of runoff for all subcatchments, σ_p^2 and $\mathrm{cov}_{p,o}$ in Equation (6) are both zero, and so ρ is undefined. The same applies to Model D. The results show that the introduction of variable rainfall produces the greatest improvement during the winter period, with correlation ρ improving from −0·317 (Model A) to 0·319 (Model B). Introduction of further complexity produces little or no improvement in stormflow volume predictions (the simulations using the most complex and fully distributed Model H and those of Model B being almost identical). These results can be explained by the fact that the soil water deficit is low in winter (or zero), so most of the effective rainfall is available for runoff generation; and as the difference between effective and actual rainfall in winter is low, the runoff patterns reflect the rainfall spatial patterns.

Therefore, accuracy of predictions of spatial patterns of stormflow volumes is dependent upon the accuracy of spatial–temporal patterns of rainfall inputs to the models. Single bucket models are adequate because the subcatchments are wet regardless of depth (within acceptable bounds); similarly, parameter variations have little effect under wet conditions (Atkinson *et al*., 2002). Yet, over the winter period, all but two of the models (Model A and Model C are exceptions) overpredict the magnitude of spatial stormflow patterns (positive values of B). The correlation between observed and predicted stormflow volumes in space over the winter period is not high, indicating there is still scope for improved prediction of spatial patterns under winter conditions.

On the other hand, the results over the summer period (see Table V) suggest that, of the three types of model improvements available (variable rainfall, variable parameters, multiple buckets), the addition of multiple buckets (Model D) provides the greatest improvement in the values of A, B and E. This improvement is a result of incorporating the effects of variable source areas, which the multiple buckets help mimic, thus providing the flexibility to predict the correct amount of saturation excess runoff. Introduction of variable rainfall alone (Model B) did improve the correlation between observed and predicted spatial patterns of stormflow volumes more than multiple buckets alone (Model D); however, the combination of variable rainfall, multiple buckets and variable parameters (Model H) provided the greatest improvement in the prediction of spatial patterns of stormflow volumes during the summer period.

These results can be explained by the high soil water deficit in summer, and the need to replenish storage before generating runoff. Therefore, the most accurate predictions of spatial patterns of stormflow volume are achieved when the catchment's soil water deficit is estimated correctly. Multiple bucket models, which incorporate a distribution of bucket sizes and can better handle variable deficits, are thus required to represent the distribution of soil water deficits accurately. The spatially variable input parameters (M, f_c and S_{bc}) have been previously shown to be important in the prediction of daily flow under dry conditions (Atkinson *et al*., 2002), and are thus clearly important in the prediction of summer stormflow volumes. However, it is only when acting in concert with variable rainfall (Model E and Model H) that variable parameters become useful in summer. These explanations, in the final analysis, tend to make Model H the best model design for summer conditions.

In summary, we found that the model complexity required to make accurate predictions of stormflow volumes varies with catchment dryness. More complex models (Model H) are required under dry summer conditions, and simple lumped representations (Model B) are adequate to make reasonable predictions under wet winter conditions. This corroborates the observations of Atkinson *et al*. (2002), who postulated that model complexity required for different regions was a function of a climatic dryness index, which in their

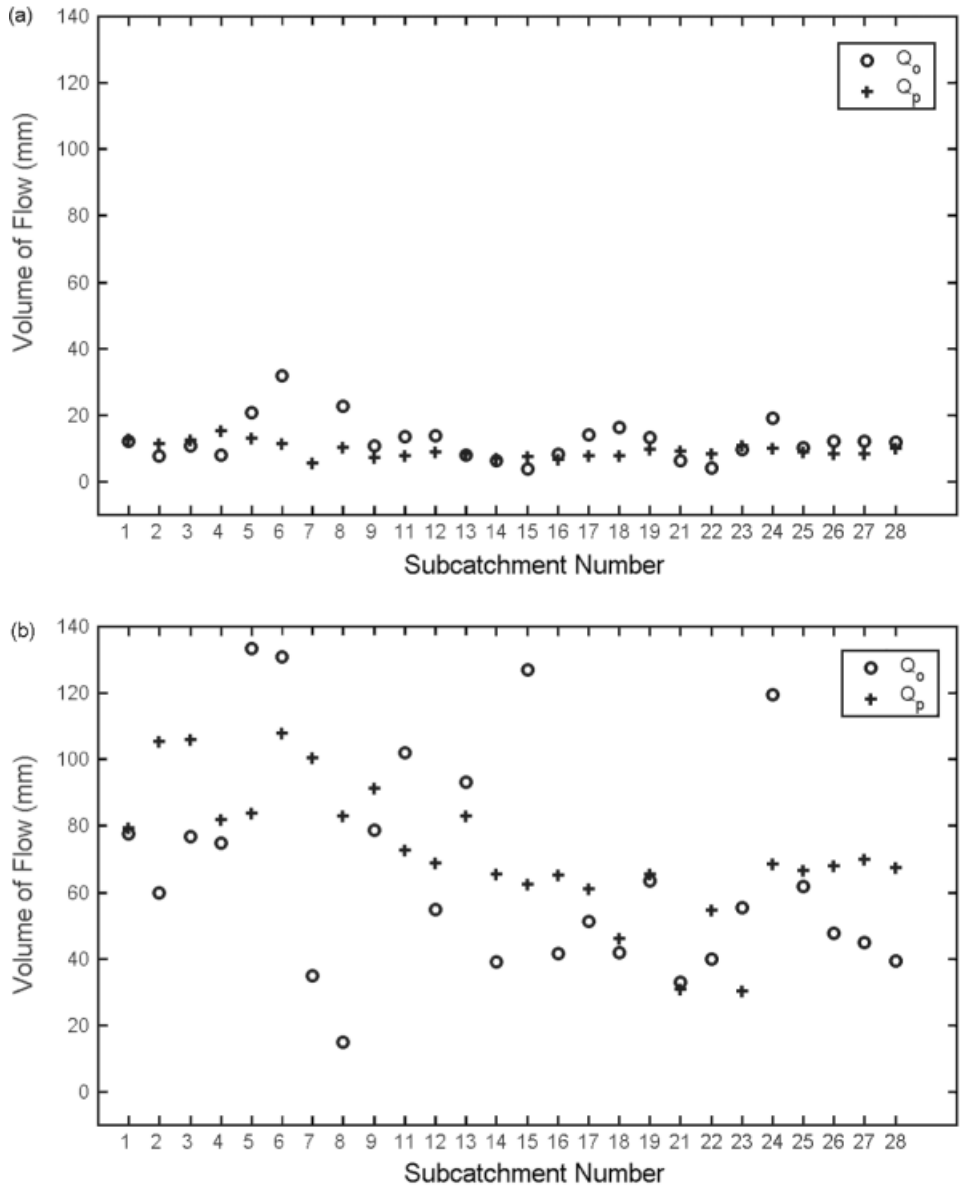

Figure 5. Observed stormflow Q_o and predicted Q_p stormflow using Model H for (a) summer and (b) winter periods

case was calculated in terms of annual totals of rainfall and potential evaporation. The results presented here suggest that this argument needs to be extended to consider *seasonal* index of dryness. However, for acceptable predictions of stormflow volumes under all seasonal conditions, at any time of the year, the more complex model (Model H) is most appropriate. Figure 5 presents the spatial patterns of stormflow volume from simulations using Model H over summer and winter periods, indicating adequate fits to observed data in summer and somewhat poorer predictions in winter. There are, however, consistent summer underpredictions and winter overpredictions, as well as fairly poor correlations between predicted and observed patterns of stormflow volume. The sources of these inconsistencies will be investigated later.

Hourly streamflow predictions

To assess the success of hourly flow predictions at all 28 gauging stations within the Mahurangi Catchment using Model H, the statistics described by Equations (3)–(6) are calculated and presented in Figure 6 for both summer and winter periods. Figure 6 also shows the means of the assessment statistics, which are indicated

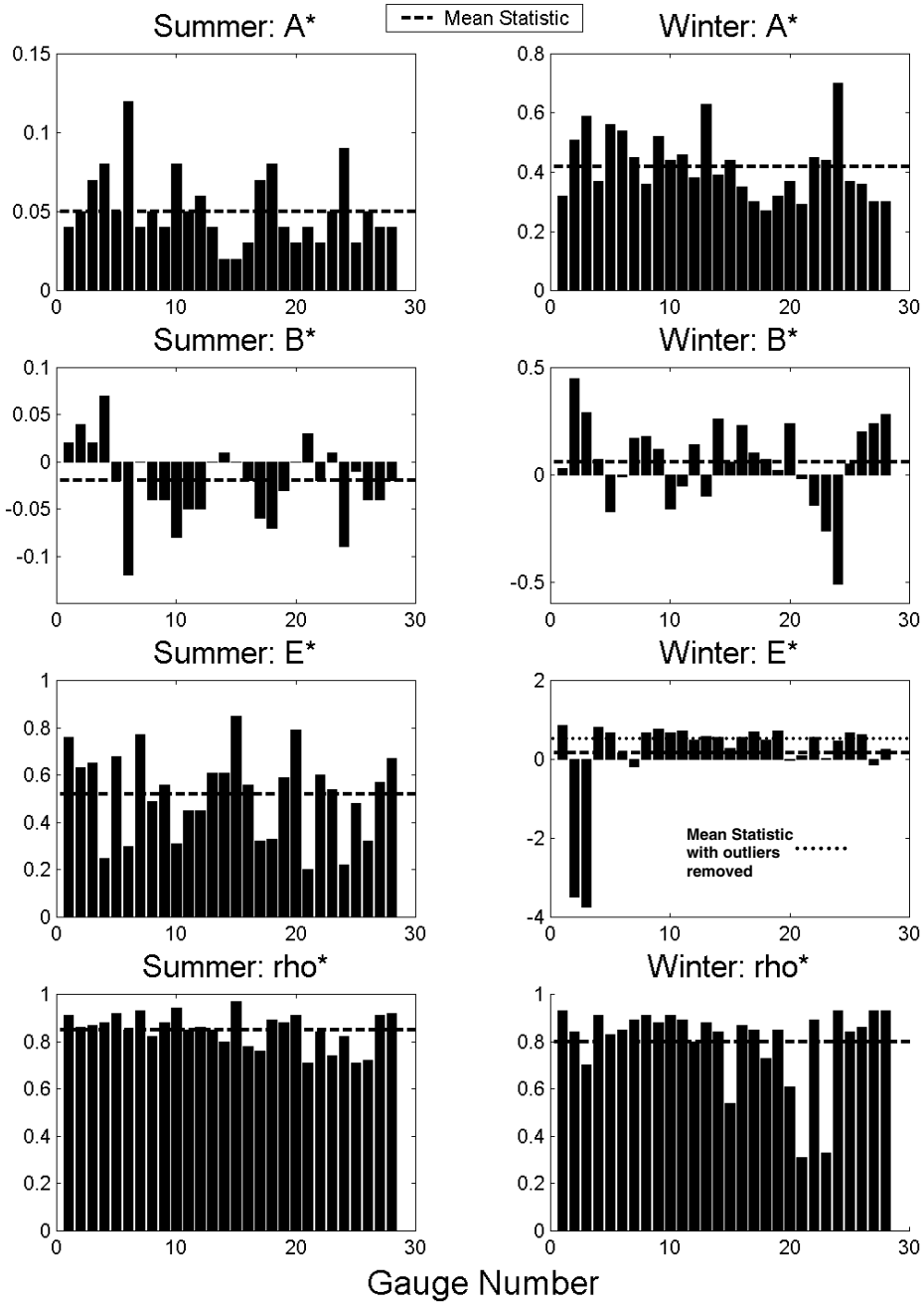

Figure 6. Goodness of fit statistics for predictions of hourly streamflow by Model H (mean absolute error A^*, mean bias B^*; efficiency E^*; correlation coefficient, at all 28 ρ^*) gauges over summer and winter periods. The broken line shows the mean statistic for the 28 gauges

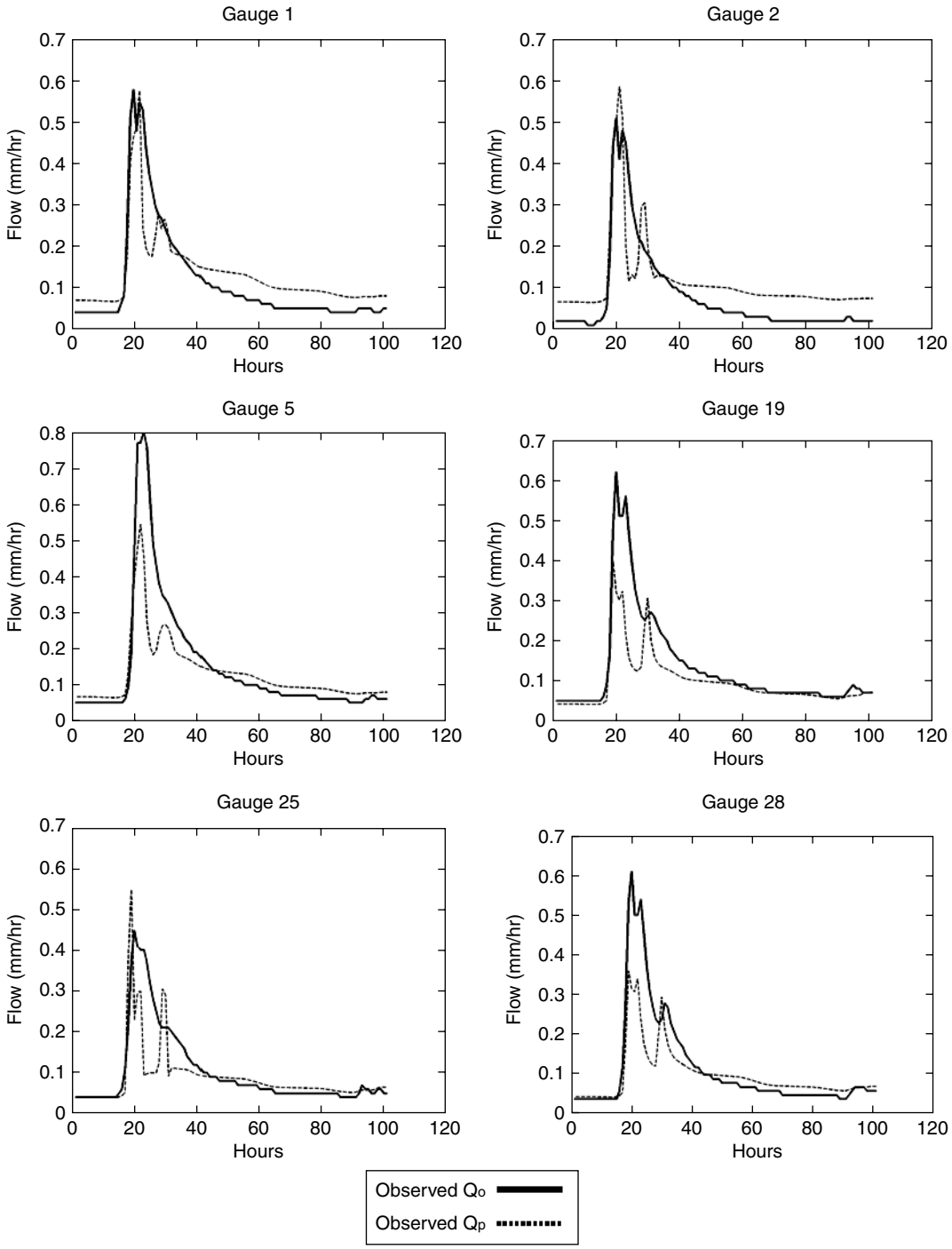

Figure 7. Observed hourly streamflow and predicted hourly streamflow using Model H over the summer period for gauges 1, 2, 5, 19, 25 and 28

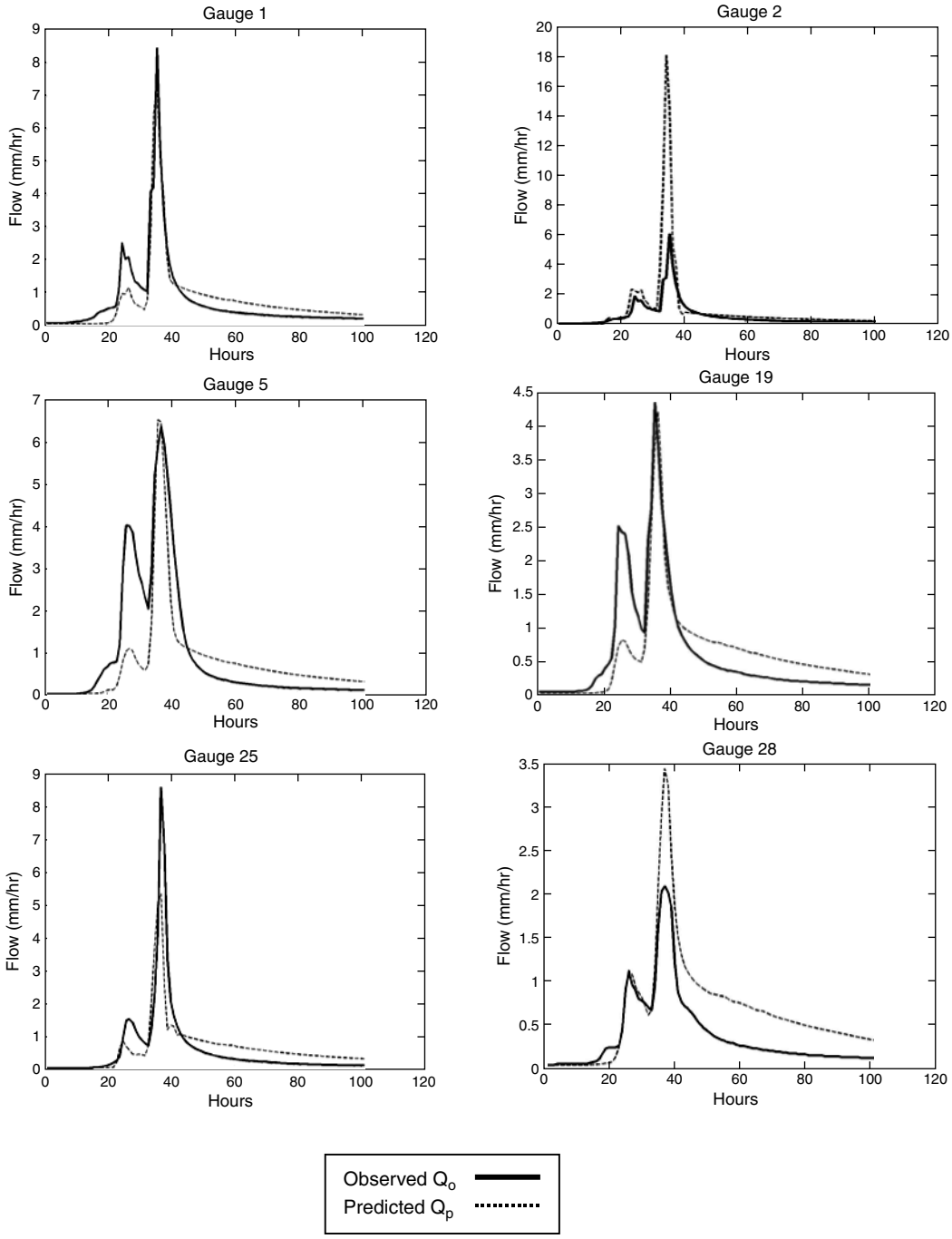

Figure 8. Observed hourly streamflow and predicted hourly streamflow using Model H over the winter period for gauges 1, 2, 5, 19, 25 and 28

by the broken horizontal lines. The results suggest that although, on average, the model makes adequate predictions of hourly streamflow across the catchment, there are winter overpredictions ($B^*_{av} = 0{\cdot}064$ mm), summer underpredictions ($B^*_{av} = -0{\cdot}021$ mm) and the correlation between observed and predicted hourly flow is moderately high (summer: $\rho^* = 0{\cdot}849$; winter: $\rho^* = 0{\cdot}805$). In addition, the predictions of peak flows are, on average, more accurate in summer than in winter (summer: $E^*_{av} = 0{\cdot}520$; winter: $E^*_{av} = 0{\cdot}173$), which is a direct result of significant winter overpredictions of stormflow volumes. Poor predictions of winter peaks (E^*) at gauges 2 and 3 are likely to be a result of gauge failure and inaccurate data filling during high flow events. As depicted in Figure 6, with the removal of the two outliers (gauges 2 and 3), the prediction of peak winter flows is improved markedly (winter: $E^*_{av} = 0{\cdot}503$).

Even with these inconsistencies, the assessment statistics suggest that, on average, the predictions of hourly streamflow in space are reasonably accurate, which is encouraging. To analyse the trends depicted in Figure 6 more closely, observed and predicted hydrographs of hourly streamflow at gauges 1, 2, 5, 19, 25, 28 from simulations using Model H (the preferred model), under both summer and winter conditions, are compared directly in Figures 7 and 8 respectively. These gauges were selected because the upstream contributing areas represent the full range of catchment properties and rainfall recorded at the Mahurangi Catchment, not because they produced the best fits. Comparison of observed and predicted hydrographs in Figures 7 and 8 highlight the magnitude of winter overpredictions, summer underpredictions and the reasonably accurate timing of peak flows. Given that the results of simulations to predict stormflow volumes indicated poor correlations of observed and predicted values and significant bias, but that hourly flow predictions demonstrated high correlations, we can deduce that the timing of the flow routing is good but that the prediction of storm volumes is the one that needs improving.

SENSITIVITY ANALYSIS

To investigate the sources of error in the timing and magnitude of runoff generated from the hillslopes of individual subcatchments depicted in Figure 3, a sensitivity analysis using Model H was performed to investigate the relative dominance of parameters assumed uniform across the catchment, and the influence that these dominant parameters have on the timing and magnitude of flow predictions. Comparison of eight models of different complexity has already identified rainfall as an important control on spatial variability of streamflow, so its effects have not been included in this sensitivity analysis, although its importance in hourly flow predictions is noted. Similarly, the results presented earlier suggest that the routing model is operating effectively and is not the source of overpredictions or poor timing. Of the remaining parameters, f_c, S_{bc} and M have been identified as dominant controls on the timing and volume of hillslope runoff (Atkinson *et al*., 2002, 2003), but we believe they have been estimated as accurately as possible through extensive field measurements, and can be omitted from any sensitivity analysis.

Therefore, the sensitivity analysis focuses on the parameters that are assumed to be homogeneous in space (between subcatchments) and these include the subsurface recession parameter a, the baseflow recession parameter T_{cbf}, the bucket distribution parameter β and the interception bucket capacity S_{bcint}. For consistency, each model parameter was varied over the same range by multiplying the mean value by 0·25, 0·5, 0·75, 1, 1·25, 1·5 and 1·75 in turn. As a result of the simulations, each parameter has seven sets of streamflow data, from which we determine the maximum spread of results by taking the difference between the maximum and minimum value of streamflow recorded in each hour and averaging over the number of hours in the selected time period. Our measure of sensitivity is the resulting mean absolute spread (in mm h^{-1}) given by

$$S = \frac{1}{n}\sum_{j=1}^{n} |q_{\max_j} - q_{\min_j}| \tag{7}$$

Here, q_{max} and q_{min} (mm h^{-1}) respectively represent the maximum and minimum hourly streamflow predictions from the seven sensitivity simulations and n is the number of hours in the selected time period.

Table VI. Sensitivity (S, mm h^{-1}) of model predictions to four model parameters using Model H in subcatchment 22

	a (mm^{1-b} h^b)	T_{cbf} (h)	β	S_{beint} (mm)
Summer period	0·1223	0·0650	0·0478	0·0162
Winter period	0·3748	0·1740	0·1733	0·0251
Process represented	Subsurface runoff	Baseflow	Surface, subsurface runoff	Interception, evaporation

The results of the sensitivity analysis will be presented for subcatchment 22. This subcatchment was selected at random. The results, over the summer and winter periods, are presented in Table VI and suggest that model predictions are very sensitive to the recession parameter a, which controls the rate of subsurface runoff, and moderately sensitive to the parameter T_{cbf}, which controls the amount of baseflow leaving the hillslope. Model simulations were less sensitive to S_{bcint} with smaller values of S. On the other hand, model predictions were insensitive to the parameter β in summer, but moderately sensitive in winter conditions due to the fact it controlled the magnitude of saturation areas and thus saturation excess runoff. As depicted by Equations (A.7) and (A.8), the a parameter has most influence on the timing of runoff from the hillslopes during periods when the soil moisture storage is high, while the baseflow parameter T_{cbf} controls the continuous volume of discharge from the hillslope. Given that parameters a and T_{cbf} have such a strong influence on the timing and magnitude of hourly flow predictions, and have been assumed homogeneous in space (when in fact they may be variable), this assumption of homogeneity is now investigated for predictions of streamflow in space and time.

Sensitivity to variations in a

It is likely that the a parameter, because of the way it is estimated from streamflow recessions at the catchment outlet, may incorporate routing effects and, therefore, may be unsuitable for predictions of flow from subcatchments upstream of the outlet. To investigate the appropriate value of a for internal flow predictions, sensitivity analysis was performed with the value of a with respect to the timing of flow predictions. The most appropriate statistic for assessing the timing of model predictions is the correlation coefficient ρ^*. Subcatchments 2, 4, 12 and 25 for the sensitivity analyses were selected because they are first-order catchments and cover all physical and climatic properties measured at the Mahurangi catchment. The sensitivity analysis varied the a parameter within $+/-2{\cdot}5$ standard deviations ($+/-2{\cdot}5\sigma$) of the mean μ by multiplying the mean value by 0·25, 0·5, 0·75, 1, 1·25, 1·5, and 1·75 in turn. The standard deviation (22·5 mm^{1-b} h^b) was estimated in the calibration exercise used to determine a. The resulting coefficient of variation CV for a is 0·3(CV $= \sigma/\mu$). Model simulations are run to produce hillslope runoff at each of the four subcatchments independently, which is then routed to the respective outlets and compared with observed streamflow. The correlation between observed and predicted streamflow ρ^* at the outlet of subcatchments 2, 4, 12 and 25 is calculated for both summer and winter periods. The results are presented in Figure 9, along with the predictions at the catchment outlet using Model H.

The results presented in Figure 9 suggest that, under both summer and winter conditions, the timing of hourly flow predictions is significantly influenced by variations in a. Decreasing a by 75% (to 18·75 mm^{1-b} h^b) improved the timing of predicted hourly flow at the outlet of each subcatchment by increasing ρ^* towards a value of unity. This improvement is more significant in summer, with ρ^* for all subcatchments exceeding that recorded for the catchment outlet. The improvement is less significant in winter, with improvement in some subcatchments and a worsening in others, compared with the predictions at the catchment outlet. Another noticeable trend is that ρ^* recorded at subcatchments 2, 12 and 25 increases with decreasing a, whereas the ρ^* estimated for subcatchment 4 is insensitive to variations in a. So, although decreasing a by 75% has improved the predictions of flow from a majority of subcatchments, this is not necessarily the optimal value. The optimal value of a is likely to vary between subcatchments and can only be identified using a

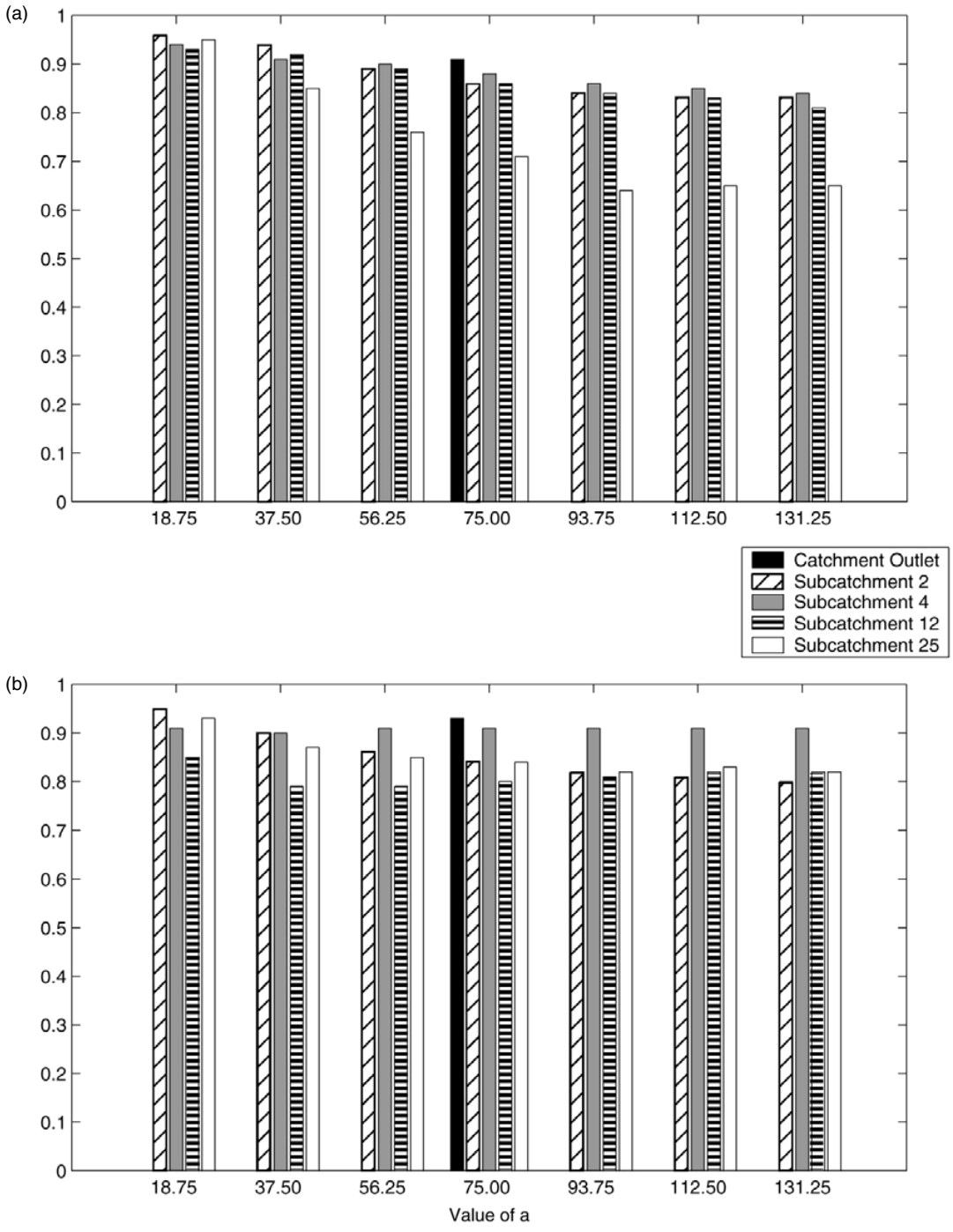

Figure 9. Sensitivity of the correlation coefficient ρ^* to variations in the recession parameter a ($\mathrm{mm}^{1-b}\mathrm{h}^b$) for subcatchments 2, 4, 12 and 25 over (a) summer and (b) winter periods. Correlation for predictions at the catchment outlet using Model H and $a = 75\mathrm{mm}^{1-b}\mathrm{h}^b$ is presented as a reference

more sophisticated sensitivity analysis than the one performed in this paper. As the recession parameter a controls the rate of subsurface discharge, where low values produce rapid catchment response, it is of no surprise that these first-order upstream subcatchments (2, 4, 12, 25), require lower values than that for the lumped catchment because they are often steeper, resulting in rapid response to rainfall, with spiky, rather than smooth, hydrographs. Therefore, a homogeneous parameter value estimated from flow at the catchment outlet is not appropriate for subcatchments further upstream, and a method is required to estimate its value in space. The parameter a can possibly be linked to physically meaningful catchment properties through the application of Darcy's law (Farmer *et al.*, 2003), and it may be possible in the future to estimate a from topography of the catchment and its soil properties. Literature research suggests accurate estimates of a have not been obtained previously from field measurements of catchment topography and soil properties, so further research in this area is required.

Sensitivity to variations in T_{cbf}

As with the a parameter, a sensitivity analysis was performed by varying T_{cbf} to investigate whether or not different values of T_{cbf} improve the total volume of predictions. We can best assess this by examining the resulting B^* statistics. Using the same subcatchments, the sensitivity analysis varied T_{cbf} within $+/-2{\cdot}5\sigma$ of the mean μ by multiplying the mean value by 0·25, 0·5, 0·75, 1, 1·25, 1·5, and 1·75 in turn. The standard deviation (600 h) was estimated in the calibration exercise used to determine T_{cbf}. The resulting coefficient of variation for T_{cbf} is 0·3 ($\mathrm{CV} = \sigma/\mu$). Model simulations are run to produce hillslope runoff at each of the four subcatchments independently, which is then routed to the gauging stations located at the respective outlets and compared with observed streamflow. The bias or the total difference in flow volume B^* was calculated for both summer and winter periods using Equation (4) for each subcatchment from the results of sensitivity analyses and is presented in Figure 10. Again, the statistics for the catchment outlet are also presented in Figure 10 to adjudge the success of the results of the sensitivity analysis.

The values of B^* presented in Figure 10 suggest that, under both summer and winter conditions, the total volume of flow predicted is strongly influenced by variations in T_{cbf}. As T_{cbf} increases, B^* decreases in summer but increases in winter, with the exception of subcatchment 4 in summer. In summer, storage is relatively low for most of the time, so much of the runoff is generated by baseflow. According to Equation (A.8), if we increase T_{cbf} then we limit the amount of baseflow, allowing the storage to increase. However, with high evaporation rates and without significant rainfall events, storage cannot increase enough to produce large amounts of subsurface flow or saturation excess runoff (if any). Therefore, increasing T_{cbf} has effectively reduced hillslope runoff, leading to underpredictions and reduced values of B^*. Conversely, decreasing T_{cbf} increases the amount of summer baseflow with little effect on the amount of subsurface runoff or saturation excess runoff produced, resulting in overpredictions of summer flows.

In winter, storage is high for most of the time; so, according to Equations (A.6) and (A.7), the majority of runoff is generated by subsurface flow or saturation excess runoff. Increasing T_{cbf} limits the amount of baseflow, so storage is allowed to increase under conditions of high rainfall and low evaporation, leading to increased rates of subsurface flow and saturation excess runoff. This increase in subsurface flow and saturation excess runoff exceeds the reduction in baseflow, leading to progressively greater overpredictions of runoff and larger, more positive, values of B^*. Conversely, decreasing T_{cbf} results in an increase in baseflow, but this increase does not compensate for the decrease in the rate of subsurface runoff or saturation excess runoff, resulting in an overall reduction in the volume of flow predicted (reducing B^*).

In summer, subcatchment 4 shows consistent overpredictions and an optimum value of T_{cbf} around 1500 to 2000 h, where B^* increases as T_{cbf} diverges in either direction. Analysis of summer rainfall patterns, summer streamflow records and values of the parameters β, f_{c} and S_{bc} shows that there is little variation between the inputs when modelling each of the four subcatchments, which could be used to explain this trend. The subcatchment does, however, have a much larger fractional forest cover ($M = 0{\cdot}6$), suggesting interception is important, especially under summer conditions. Therefore, it is possible that an underprediction

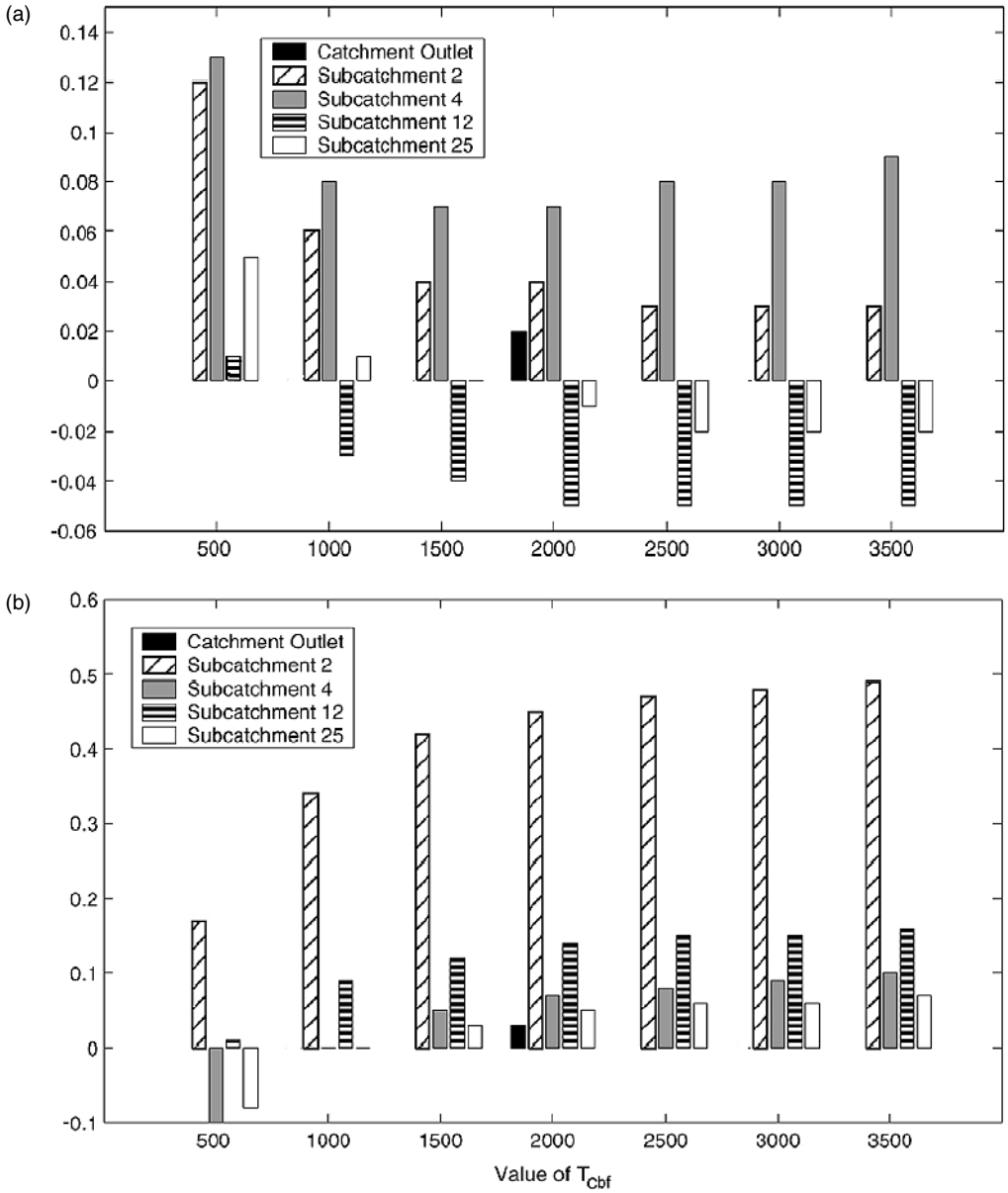

Figure 10. Sensitivity of the bias B^* (mean difference in observed and predicted volumes) to variations in the baseflow parameter T_{cbf}(h) for subcatchments 2, 4, 12 and 25 over (a) summer and (b) winter periods. Bias for the catchment outlet using Model H and $T_{cbf} = 2000$ h is presented as a reference

of the amount of interception may be responsible for consistent overpredictions of summer streamflow from subcatchment 4 through excessive throughfall. Assuming this is the case, increased throughfall raises the modelled storage above the observed in the field (or observed at subcatchments 2, 12 and 25), increasing the occurrence of predicted runoff via subsurface runoff and saturation excess mechanisms. However, under dry summer conditions, throughfall is only enough to raise storage at or around the threshold storage S_{fc}, rather than the levels experienced throughout winter. Therefore, any large decrease in T_{cbf} will produce more

baseflow and less subsurface flow, whereas any large increase in T_{cbf} will produce more subsurface flow but less baseflow. As S_{fc} governs the transition between subsurface flow and baseflow, and given that storage never exceeds S_{fc} by any large amount, the two volumes of runoff produced by increasing and decreasing T_{cbf} are similar. The 'optimum value' of T_{cbf} occurs where neither large amounts of baseflow nor large amounts of subsurface runoff are produced ($1500 < T_{cbf} < 2000$ h). Inclusion of seasonal variations in leaf area index (LAI) or interception capacity, or even a detailed sensitivity analysis, may provide some insight into this problem—these have not been conducted in this paper and warrant further consideration.

Although an optimal value of T_{cbf} has not been identified, the value of B^* calculated from all subcatchments under both summer and winter conditions can be improved by either increasing or decreasing T_{cbf} in the range of $+/-\sigma$. In most cases, B^* can be reduced to zero or to a value lower than that recorded at the catchment outlet by varying T_{cbfj} however, there are instances where this is not the case (e.g. subcatchment 2 in winter, where an optimum value less than 500 h is suggested). For these subcatchments, the accuracy of input information, such as rainfall and parameter values, requires closer examination. However, in general, the results of sensitivity analysis suggest that the assumption of a uniform value for T_{cbf} across the catchment is not appropriate and estimates of T_{cbf} for each individual subcatchment are required to improve internal predictions of hourly streamflow. Observed streamflow records across the catchment show strong variations in the amount of baseflow occurring at different locations around the catchment (in some instances there is almost no baseflow), so it is not surprising to find that we require spatially variable values of T_{cbf} to improve the volume of flow predictions within the catchment. Therefore, as with the a parameter, a method is required for the *a priori* estimation of the spatial patterns of T_{cbf}. Instead of being resigned to the fact that these parameters can only be estimated by calibration, future research should endeavour to establish links between estimates of these drainage parameters (obtained from recession curve analysis or tracer techniques) with catchment physical attributes, such as topography, soils, vegetation, and hydrogeology, and in this way permit the eventual *a priori* specification of these parameters in models.

CONCLUSIONS

The aim of the paper was not to present a model that can be used for hourly predictions. Rather, it was to investigate the level of complexity needed in models for making space–time predictions of streamflow at the hourly time scale. We tested eight different configurations of model complexity, all of which had the same building block. This testing took the form of learning from observed patterns of streamflow variability in space and time through systematic application of this hierarchy of models. The testing of the eight models with different complexities does not identify one distinct path that should be used when attempting to identify the most suitable model. However, it does allow comparison of the results of simple 'lumped' models against more complex models, which enables us to deduce the accuracy of models with increasing complexity and make the connection between climate controls, time scale and model performance. In spite of the poor quality of some of the observations, which prevented a proper evaluation of the models' ability to reproduce the observations, considerable insights have been obtained through our analyses that will be highly useful in future modelling efforts.

Systematic analysis of eight models with different complexity (but based on the same simple model configuration) has found that the model complexity required to predict spatial patterns of stormflow volumes across the Mahurangi Catchment varies with season (winter versus summer). This result supports the conclusions drawn by Atkinson *et al.* (2002, 2003), where model complexity was found to be a function of time scale and the climatic dryness index (ratio of annual potential evaporation to annual precipitation). During winter periods the soils are wet and accurate predictions of stormflow are achieved using lumped models with catchment average parameter values, a single bucket/store and spatially variable rainfall (Model B). Conversely, during summer periods the soils are dry, and complex and fully distributed models with spatially variable rainfall and input parameters and multiple buckets are required for accurate predictions of

stormflow (Model H). The inclusion of multiple buckets, and thus the effects of variable source areas, was found to be the most important of the three additions to model complexity, providing the flexibility to predict the correct amount of saturation excess runoff over both summer and winter periods. Analysis of observed patterns of total rainfall and stormflow during summer and winter periods suggests that the level of model complexity required is dependent on how well the soil water deficit is modelled.

The systematic analysis of models with different complexity presented in this paper has demonstrated that, under all seasonal conditions, model performance generally improves with increasing model complexity and spatial discretization. It has also allowed identification of the most appropriate design, and has provided us with significant insights into the relative importance of catchment properties, their spatial variability, and their influence on spatial and temporal flow variabilities across the catchment. Sensitivity analysis has given additional insights into the dominant controls on variability, and thus the validity of the assumption of homogeneity of a number of catchment properties and attributes. On average, reasonably accurate predictions of hourly flow across the Mahurangi Catchment can be achieved using the final (recommended) fully distributed Model H and the data available. However, more accurate internal predictions are possible with more precise estimates of the subsurface recession parameter a and the baseflow parameter T_{cbf} in space. This topic requires further investigation, and a consistent method of parameter estimation is desirable. The parameter β may remain homogeneous in summer, because variations in its value did not significantly affect the timing or magnitude of hourly predictions, whereas heterogeneity of β was important for accurate predictions for winter flows. Although the type of hydrological model used in this paper is site specific, a similar approach could be taken at different sites, if the fundamental runoff generating mechanisms have been represented well in an appropriate model.

ACKNOWLEDGEMENTS

The staff of the National Institute of Atmospheric Research, New Zealand, are thanked for providing all data and information needed for this study, and for their continued support and encouragement. The first author was supported by an Australian Postgraduate Award provided by the Commonwealth Government of Australia. CWR Reference ED 1587 SA.

APPENDIX A

Notation

S_{bc}	bucket capacity (mm)
D	soil depth (mm)
ϕ	porosity (dimensionless)
θ_{fc}	field capacity (dimensionless)
θ_{pwp}	permanent wilting point (dimensionless)
f_{c}	threshold storage parameter (dimensionless)
S_{fc}	threshold storage (mm)
E_{veg}	transpiration (mm h^{-1})
E_{bs}	bare soil evaporation (mm h^{-1})
E_{p}	potential evaporation (mm h^{-1})
E_{int}	evaporation from interception store (mm h^{-1})
M	fractional forest cover (dimensionless)
$S(t)$	storage (mm h^{-1})
S_{int}	interception storage (mm)
Q_{ss}	subsurface runoff (mm h^{-1})

Q_{se}	saturation excess runoff (mm h^{-1})
a	non-linear discharge parameter (mm^{1-b} h^b)
b	non-linear discharge parameter (dimensionless)
Q_{bf}	baseflow (mm h^{-1})
T_{cbf}	baseflow response time (h)
ρ	correlation between predicted and observed streamflow (dimensionless)
A	mean absolute error (mm)
B	mean bias (mm)
E	efficiency (dimensionless)
S	sensitivity (mm h^{-1})
β	empirical parameter describing the distribution of buckets (dimensionless)
S_{bcint}	interception bucket capacity (mm)
T	throughfall (mm h^{-1}), water in excess of interception bucket capacity

Model equations

Bucket capacity

$$S_{bc} = D(\phi - \theta_{pwp}) \tag{A.1}$$

Threshold storage parameter and threshold storage

$$f_c = \frac{(\theta_{fc} - \theta_{pwp})}{(\phi - \theta_{pwp})} \tag{A.2}$$

$$S_{fc} = S_{bc} f_c \tag{A.3}$$

Transpiration

$$E_{veg} = ME_p \qquad \text{if } S(t) \geq S_{fc} \tag{A.4}$$

$$E_{veg} = ME_p \left(\frac{S(t)}{S_{fc}}\right) \qquad \text{if } S(t) < S_{fc}$$

Bare soil evaporation

$$E_{bs} = E_p(1 - M) \qquad \text{if } S(t) \geq S_{bc} \tag{A.5}$$

$$E_{bs} = E_p(1 - M) \left(\frac{S(t)}{S_{bc}}\right) \qquad \text{if } S(t) < S_{bc}$$

Saturation excess

$$Q_{se} = 0 \qquad \text{if } S(t) \leq S_{bc} \tag{A.6}$$

$$Q_{se} = S(t) - S_{bc} \qquad \text{if } S(t) > S_{bc}$$

Sub-surface runoff (Wittenberg and Sivapalan, 1999)

$$Q_{ss} = 0 \qquad \text{if } S(t) < S_{fc} \tag{A.7}$$

$$Q_{ss} = \left(\frac{S(t) - S_{fc}}{a}\right)^{1/b} \text{if } S_{fc} < S(t) < S_{bc}$$

$$Q_{ss} = \left(\frac{S_{bc} - S_{fc}}{a}\right)^{1/b} \text{if } S(t) > S_{bc}$$

Baseflow (Atkinson *et al*., 2002)

$$Q_{\mathrm{bf}} = \left(\frac{S(t)}{T_{\mathrm{cbf}}}\right) \qquad \forall t, S(t) \tag{A.8}$$

Interception

$$E_{\mathrm{int}} = E_{\mathrm{p}} \qquad \text{if } P + S_{\mathrm{int}}(t) \geq E_{\mathrm{p}} \tag{A.9}$$

$$E_{\mathrm{int}} = P + S_{\mathrm{int}}(t) \qquad \text{if } P + S_{\mathrm{int}}(t) < E_{\mathrm{p}}$$

Total actual evaporation

$$E_{\mathrm{total}} = E_{\mathrm{veg}} + E_{\mathrm{bs}} + E_{\mathrm{int}} \tag{A.10}$$

Water balance for interception store

$$S_{\mathrm{int}}(t+1) = S_{\mathrm{int}}(t) + P - E_{\mathrm{int}} - T \tag{A.11}$$

Water balance for soil water

$$S(t+1) = S(t) + P + S_{\mathrm{int}}(t) - S_{\mathrm{int}}(t+1) - E_{\mathrm{veg}} - E_{\mathrm{bs}} - E_{\mathrm{int}} - Q_{\mathrm{se}} - Q_{\mathrm{ss}} - Q_{\mathrm{bf}} \tag{A.12}$$

Throughfall

$$T = P - S_{\mathrm{bc}} \qquad \text{for } P > S_{\mathrm{bcint}} \tag{A.13}$$

REFERENCES

Abbott MB, Bathurst JC, Cunge JA, O'Connell PE, Rasmussen J. 1986. An introduction to the European Hydrological System—Système Hydrologique Européen, "SHE", 1: history and philosophy of a physically-based, distributed modelling system. *Journal of Hydrology* **87**: 45–59.

Atkinson SE, Woods RA, Sivapalan M. 2002. Climate, soil, vegetation controls on water balance model complexity over changing timescales. *Water Resources Research* **38**(12): 1314, doi: 10.1029/2002 WR001487.

Atkinson SE, Sivapalan M, Woods RA, Viney NR. 2003. Dominant physical controls on hourly flow predictions and the role of spatial variability: Mahurangi Catchment, New Zealand. *Advances in Water Resources* **26**: 219–235.

Duncan MJ. 1995. Hydrological impacts of converting pasture and gorse to pine plantation, and forest harvesting, Nelson, New Zealand. *Journal of Hydrology (New Zealand)* **34**(1): 15–41.

Eder G, Sivapalan M, Nachtnebel HP. 2003. Modelling water balances in an Alpine catchment through exploitation of emergent properties over changing time scales. *Hydrological Processes* **17**: 2125–2149.

Farmer D, Sivapalan M, Jothityangkoon C. 2003. Climate, soil and vegetation controls upon the variability in temperate and semi-arid landscapes: downward approach to hydrological analysis. *Water Resources Research* **39**(2): 1035, doi: 10.1029/2001 WR000328.

Hughes DA, Smakhtin V. 1996. Daily flow time series patching or extension: a spatial interpolation approach based on flow duration curves. *Hydrological Sciences Journal* **41**(6): 851–871.

Ibbitt RP, Henderson RD. 1998. Filling in missing data in flow records. In *Proceedings, International Symposium on Hydrology, Water Resources and Environmental Development and Management in Southeast Asia and the Pacific*, Department of Civil Engineering, Yeungnam University, 214-1 Daedong, Kyongsan, Republic of Korea; 712–749.

Jothityangkoon C, Sivapalan M, Farmer DL. 2001. Process controls of water balance variability in a large semi-arid catchment: downward approach to hydrological modelling. *Journal of Hydrology* **254**: 174–198.

Klemes V. 1983. Conceptualisation and scale in hydrology. *Journal of Hydrology* **65**: 1–23.

Moore ID, Grayson RB. 1991. Terrain based prediction of runoff with vector elevation data. *Water Resources Research* **27**(6): 1177–1191.

Viney NR, Sivapalan M. 1995. *LASCAM: the large scale catchment model: user manual*. Report No. WP 1070 NV, Centre for Water Research, Nedlands, Western Australia.

Wittenberg H, Sivapalan M. 1999. Watershed groundwater balance estimation using streamflow recession analysis and baseflow separation. *Journal of Hydrology* **219**: 20–33.

Woods RA, Grayson RB, Western AW, Duncan MJ, Wilson DJ, Young RI, Ibbitt RP, Henderson RD, McMahon TA. 2001. Experimental design and initial results from the Mahurangi River Variability Experiment: MARVEX. In *Land Surface Hydrology, Meteorology and Climate: Observations and Modelling*, Lakshmi V, Albertson JD, Schaake J (eds). *Water Science and Application, American Geophysical Union*, Volume 3. AGU: Washington, DC; 201–213.

Ye W, Bates B, Viney NR, Sivapalan M, Jakeman AJ. 1997. Performance of conceptual rainfall-runoff models in low-yielding ephemeral catchments. *Water Resources Research* **33**: 153–166.

Zhao RJ, Zhang YL, Fang LR, Liu XR, Zhang QS. 1980. The Xinanjiang model. In *Hydrological Forecasting*. IAHS Publication, **129**. IAHS Press: Wallingford: 351–356.

